

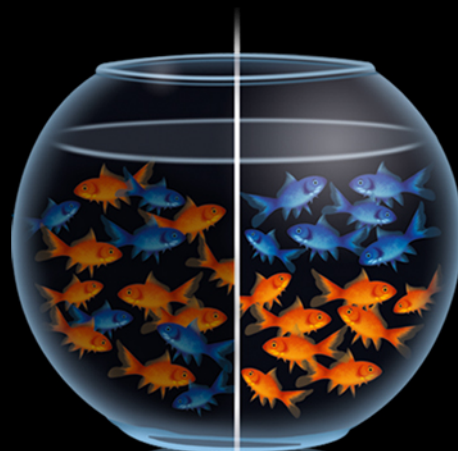
# rapidFLIM<sup>HiRes</sup>

Redefining standards for dynamic FLIM imaging

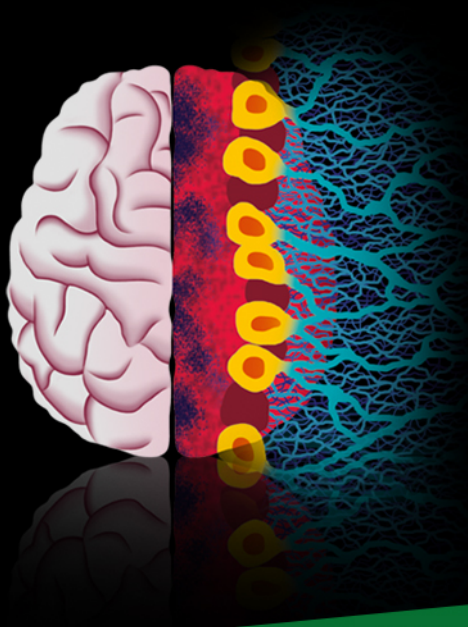


**SEE THE  
CHANGE.**

**SEE IT  
PRECISELY.**



**SEE IT  
CONFOCAL.**



**DOWNLOAD Free White Paper**



PICOQUANT

# *In-situ* SEM observation of grain growth in the austenitic region of carbon steel using thermal etching

R. HEARD , K.I. DRAGNEVSKI  & C.R. SIVIOUR   
Solid Mechanics Group, Department of Engineering Science, University of Oxford, Oxford, UK

**Key words.** *In-situ* scanning electron microscopy (SEM), abnormal grain growth, austenite, heat treatment.

## Summary

A novel heat stage, recently developed for use within the Scanning Electron Microscope, has facilitated Secondary Electron imaging at temperatures up to 850°C. This paper demonstrates one of the applications of *in-situ* elevated temperature Scanning Electron Microscope imaging: observation and quantification of grain growth within the austenitic region of carbon steels. The resulting Secondary Electron data have used the technique of thermal etching to capture possible 'abnormal grain growth' in the austenitic region. Previous *ex-situ* and post-heating results from carbon steels indicate normal, non-linear grain growth. Therefore, this new dataset provides greater insight into the heat treatment of steels. From comparison of the *in-situ* data with the overall grain growth, measured *ex-situ*, it is further concluded that abnormal grain growth is representative of the growth at temperature. Thus, the heating and cooling parts of the heat treatment are likely to account for the non-linearity previously documented in *ex-situ* results and, hence, the range of powers recorded when fitting power law models for steel grain growth. The ability of data derived from *in-situ* thermal etching to represent the microstructure of the entire surface and the bulk material is also considered.

## Introduction

Heat treatment of steel plays a vital role in the control of microstructure and the subsequent mechanical properties. It is well known that grain growth correlates to heat treatment parameters including time and temperature and, also, controls subsequent physical and mechanical properties (Sisson, 2001). It is widely accepted that grain growth over time can be modelled by the general power law equation (Eq. (1)), originally derived by Burke and Turnbull (1952)

$$d^n - d_0^n = Kt, \quad (1)$$

where  $d$  is the average grain diameter at a given time  $t$ ,  $d_0$  is the grain diameter at  $t = 0$ , and  $K$  and  $n$  are material parameters.

However, this aspect of microstructural evolution has not been tracked *in-situ*. *Ex-situ* studies on carbon steel post-heat treatment report a variety of  $n$  values between 2 and 8 (Lasagni *et al.*, 2008). Subsequent attempts at modelling have had reasonable success in predicting the growth within the austenitic region of carbon steels based on a combination of thermal modelling and *ex-situ* data (Lee & Lee, 2008). Recent, *in-situ*, high temperature studies of steel have examined the ferrite to austenite phase change using EBSD. Such studies have carried out cyclic austenite–ferrite phase transformations of a few localized grains, which demonstrates ferrite grains shrinking as austenite grains grow during the transformation (Farahani *et al.*, 2019). However, there is little understanding about microstructural evolution of the grain size during the ferrite to austenite phase change as well as once the microstructure is fully austenitic.

In the current paper, the use of an *in-situ* heat stage has facilitated examination of steel grain growth within the austenitic region at temperatures up to 850°C observed via *in-situ* thermal etching. Thermal etching is the development of surface etches at grain boundaries through exposure to elevated temperatures. The grain boundaries impinge on the specimen surface; because of equilibration of the triple junction between the grain boundary and the free surface, the surrounding specimen surface rises away from the boundary (Mullins, 1986). Compared to EBSD, the use of thermal etching combined with Scanning Electron (SE) imaging allows examination of a larger number of grains, with the aim, in this study, of giving a quantitative representation of the grain growth. The heat treatment in this study is equivalent to those used in commercial heat treatment processes (Dossett & Boyer, 2006), with the exception of the required sample preparation. The study further compares the *in-situ* surface observations to *ex-situ* data obtained on the surface and within the bulk of the specimen after cooling. This allows quantification of the effect of thermal etching on the grain growth observed *in-situ*.

## Materials and methods

An *in-situ* investigation into the grain growth within the austenitic region of 0.4% carbon steel was carried out within a

Correspondence to: R. Heard, Solid Mechanics Group, Department of Engineering Science, University of Oxford, Trinity College, Broad Street, Oxford, OX1 3BH, England. Tel: 01865 2 73098; e-mail: rhiannon.heard@trinity.ox.ac.uk

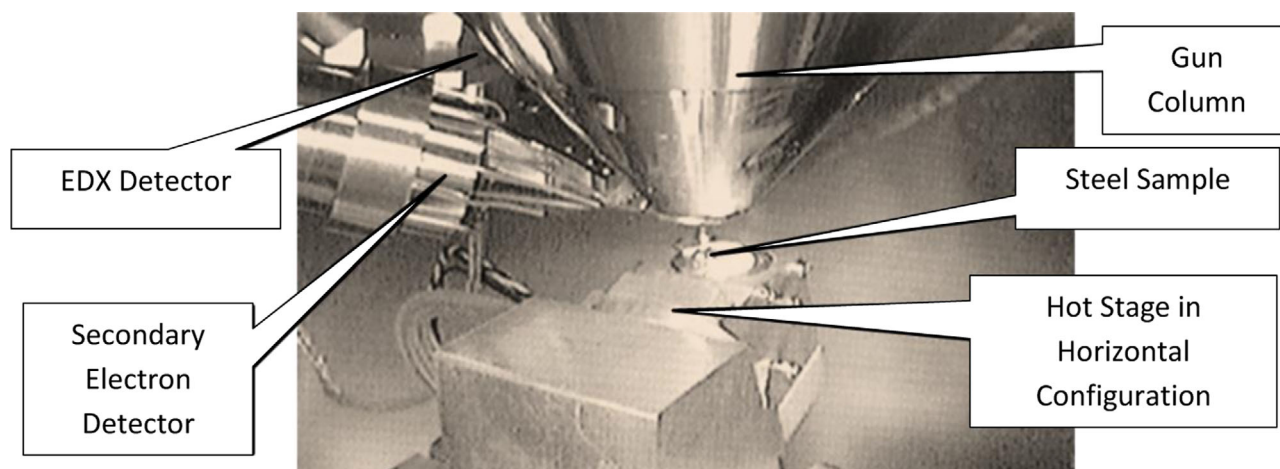


Fig. 1. Hot stage mounted within a Carl Zeiss Evo VP-SEM.

Carl Zeiss Evo Scanning Electron Microscope. A rod of BS970 carbon steel in its bright, drawn condition was normalized by heating within a furnace for 1 h at 850°C before air cooling. Disk samples of diameter 8 mm and thickness 2 mm were cut from the rod. Samples were then prepared by grinding, using progressively finer silicon carbide papers (grades: P240, P400, P600, P800 and P1200), and then polishing, firstly using three grades of diamond suspension (9, 3 and 1  $\mu\text{m}$ ) and finally colloidal silica (0.07  $\mu\text{m}$ ) combined with a water-based miscible polishing lubricant. This sample preparation produced a smooth surface, which is required to facilitate thermal etching during heating (Mullins, 1986) in the SEM vacuum chamber. The sample was mounted onto a specially designed heat stage, developed in collaboration with Deben UK Ltd, and inserted into the SEM (Fig. 1) (Heard *et al.*, 2020). The heat stage is based on a molybdenum button heater and allows imaging up

to 920°C without the need for shielding. The conditions for imaging were 15 kV electron beam with a LaB6 crystal source in a vacuum of  $9 \times 10^{-5}$  mbar at a magnification of 2 kx and working distance of 12 mm.

The sample was heated to 800°C at an approximate heating rate of  $1^\circ\text{C s}^{-1}$  and held at this temperature, which is in the austenitic region, for 45 min, before being allowed to cool in vacuum. The cooling process took approximately 60 min. This is representative of the methodology used for normalizing of steel (Treating, 2006). The austenitic region was determined using the Iron–Carbon phase diagram: the steel is 0.4 wt% C (Ngan, 2019). Figure 2 shows a schematic of the full heat treatment process. SE images were captured at 800 °C as soon as the sample surface reached temperature, and after 10, 20, 30, 40 and 45 min at temperature to observe any change in microstructure during this time. From the SE images

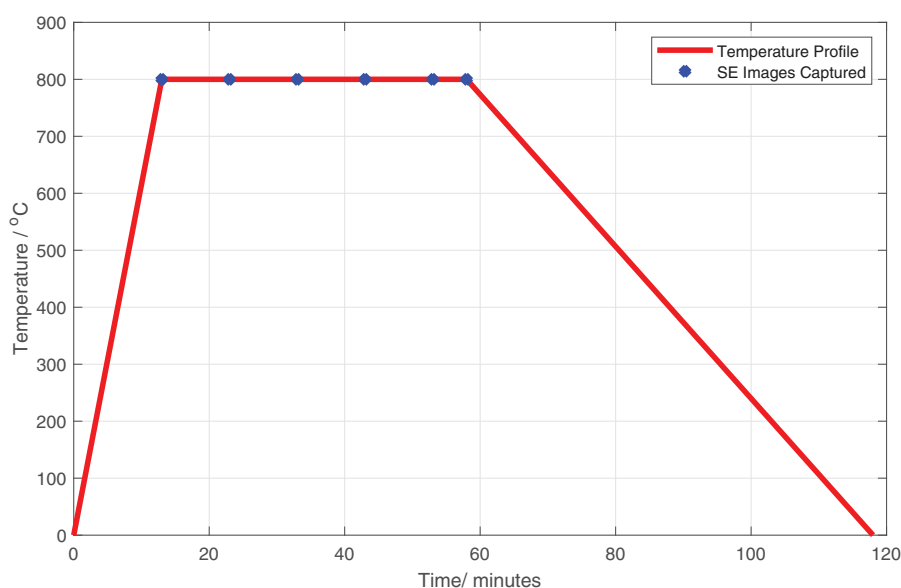


Fig. 2. Schematic diagram of heat treatment process of the carbon steel within the SEM.



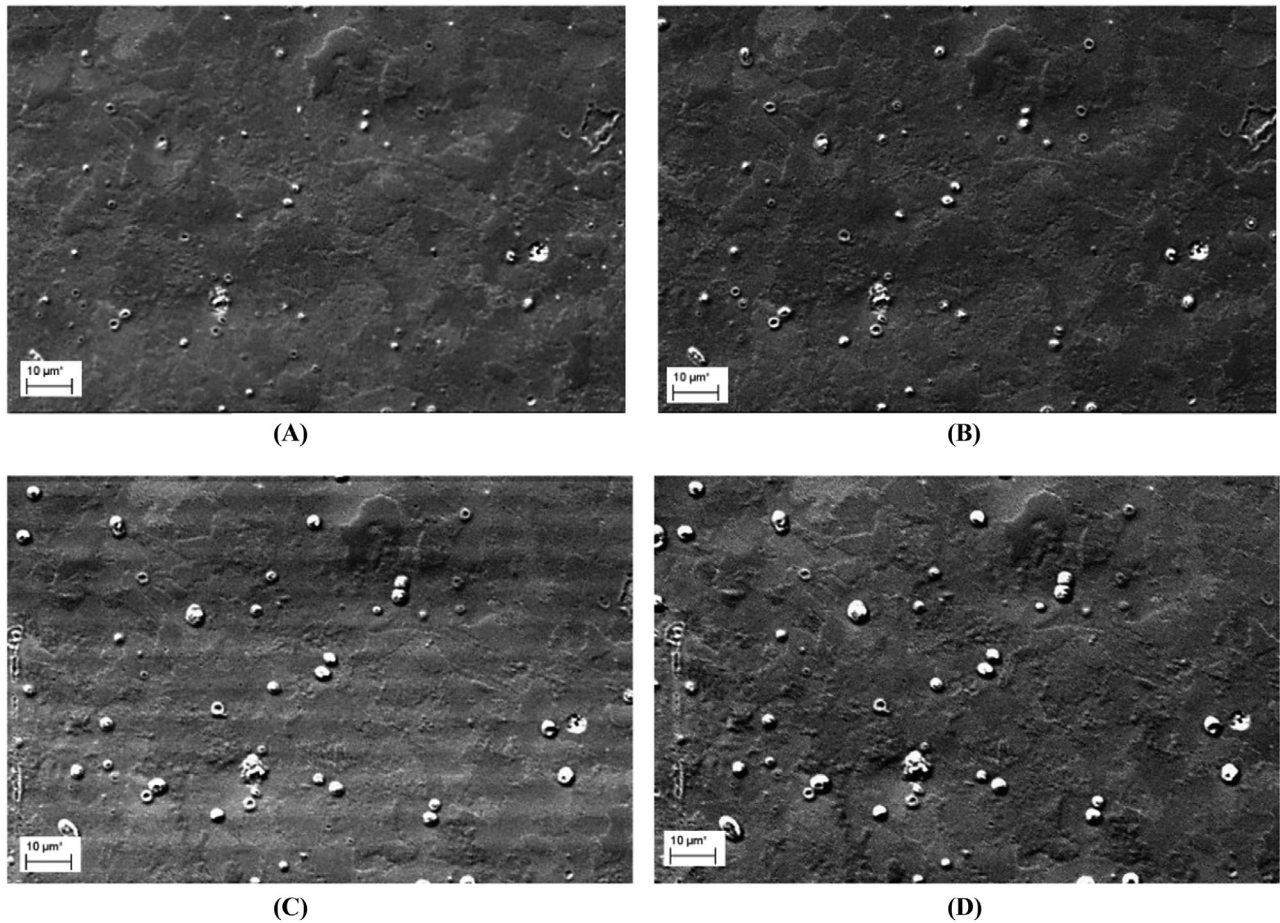


Fig. 3. SE images of thermally etched carbon steel at 800°C showing progression of grain growth at (A) time = 0 min, (B) 10 min, (C) 30 min (D) 45 min.

taken at 800 °C, it was possible to track the grain growth at temperature as a result of thermal etching (Mullins, 1986). In this experimental case, grain boundaries became visible at 700°C during the heating process, enabling *in-situ* observation.

Post-experimental analysis comprised of manually detecting grain boundaries by visual observation and outlining using the drawing and analysis software ImageJ (Schneider *et al.*, 2012). The mean grain area was found using the Planimetric method, by counting the total number of grains in a given area, following ASTM Standard E112 (Methods, 2013), for each SEM image. The mean grain diameter at each time interval was then calculated from the average area using the equivalent circular area diameter method (Li *et al.*, 2005), represented by Eq. (2).

$$d = \sqrt{4a/\pi}, \quad (2)$$

where  $d$  is the equivalent circular area diameter and  $a$  is the measured mean grain area. The power law equation, Eq. (1), was then fit to the data for grain growth over time at 800°C.

One possible concern when using thermal etching as a grain growth quantification technique is the potential effect of the

etching itself on grain boundary mobility. To better understand this, the surface and bulk microstructures were compared post-heating using a chemical etch. To facilitate chemical etching, samples were polished with 9, 3 and 1 µm diamond solution before applying a 2% Nital etchant for 70 s. The sample surface was then imaged using the optical microscope of an Alicona Profilometer at magnifications of 5×, 20×, 50× and 100×. The 50× magnification images were used to calculate the average grain size using the Planimetric method as described above. The sample bulk was subsequently characterized by grinding down 0.5 mm of the sample from the surface and then repeating the polishing, etching and imaging.

## Results

The SE images, Figure 3, of the steel obtained at 800°C, over a time period of 45 min, enabled the evaluation of grain size evolution in the austenitic region; a previously undocumented measurement. The grains can be clearly identified in the SE images of the thermally etched specimen; these were used for grain growth quantification. The results also show

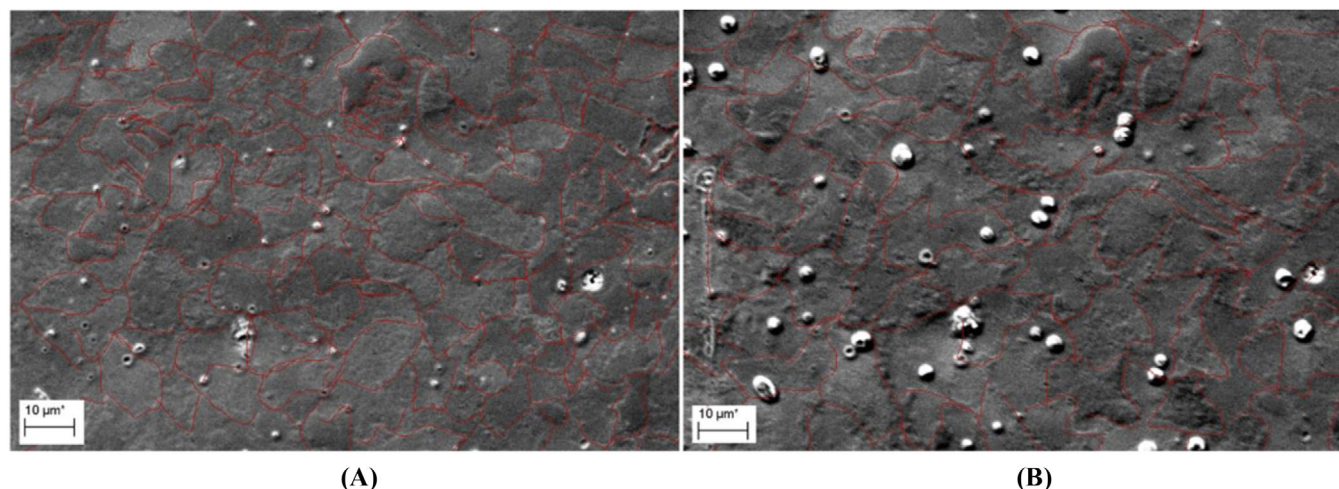


**Fig. 4.** SEM images at 800 °C after (A) 0 min and (B) 45 min. The red lines identify the grain boundary locations, identified by the thermal etch and outlined in ImageJ (Schneider *et al.*, 2012).

some residual silica from sample preparation (white spots) which become more apparent with increasing time. Unfortunately, Figure 3C shows some noise in the form of horizontal lines across the image. This is attributed to electrical interference from the heating stage, but only occurs when there is a slight temperature change, by 1°C or 2°C, and hence, a change in voltage occurs to return the stage to the set temperature. The interference is minimal and does not affect the ability to collect quantifiable data; however, it is unavoidable if it is desired to capture SE data at regular time intervals.

The grain boundaries were outlined manually using ImageJ (Schneider *et al.*, 2012) and the average grain area calculated using the Planimetric method; outlined grain boundaries at 800 °C at times of 0 and 45 min are shown in Figure 4. These were analysed using the equivalent circular diameter method to produce diameters, Figure 5. These data were, in turn, used to fit the general power law equation. The data give a linear relationship between time and grain growth; the general power law constants are  $n = 1$  and  $K = 0.054 \mu\text{m}^n\text{min}^{-1}$ .

To determine how representative the *in-situ* data were of the whole sample, as well as any disparities between the bulk

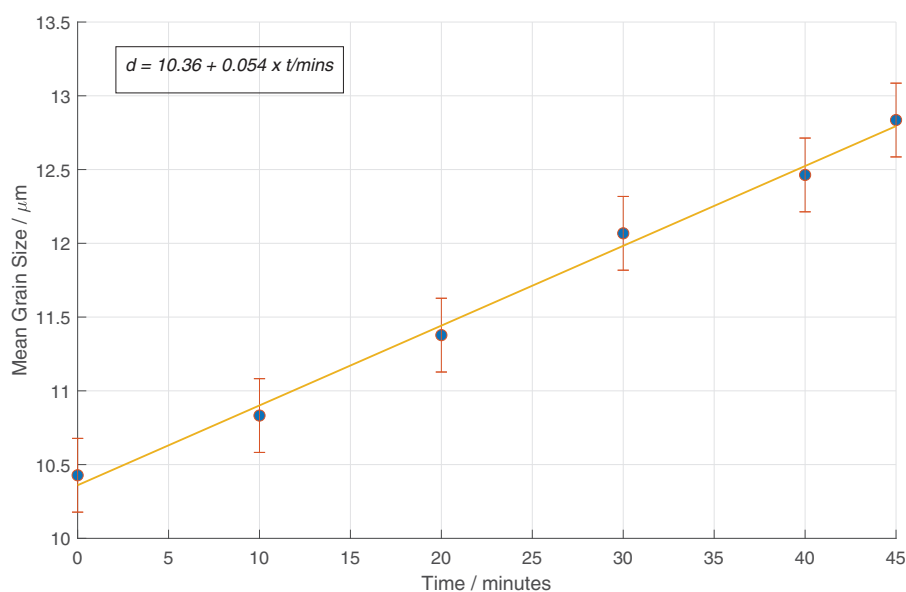


**Fig. 5.** Mean grain size of carbon steel at 800°C as a function of time; an error bar of  $\pm 0.25 \mu\text{m}$  is shown for each data point as standard for the ASTM Standard E112 Planimetric method (Methods, 2013). Observable grains within each SEM image are shown in the Appendix: at least 90 grains for each image.



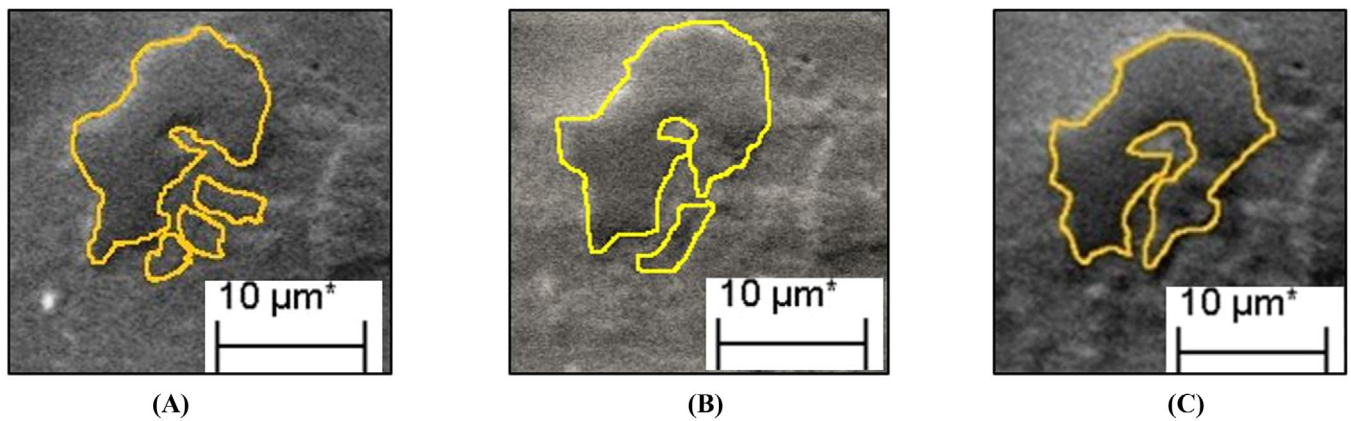


Fig. 6. SE images at 800 °C depicting abnormal grain growth at (A) 0 min, (B) 20 min and (C) 45 min.

and surface of the sample and effects of heating and cooling, *ex-situ* data were collected. Optical images were captured pre- and post-heating of the surface and bulk of the sample and the grain sizes compared to the *in-situ* data; as shown in Figure 5. Figure 5A presents the grain sizes calculated from the *in-situ* at images at the time the sample surface reached 800 °C and after 45 min of heating at this temperature. Figure 5B shows a summary of the *ex-situ* grain size results of the surface before and after heating and in the bulk after heating. Comparison between the *ex-situ* and *in-situ* data indicate that most of the grain growth occurs within the 45 min of heating at 800 °C as the difference in grain size on the surface after 45 min at 800 °C and post-cooling is negligible under these conditions. Similarly, the grain size calculated *in-situ* as the temperature reached 800 °C is comparable to that *ex-situ* before heating, although it is possible some minor grain growth occurred during heating. Additionally, Figure 5B also indicates that the grain size on the surface post-heating is representative of the overall microstructure within the bulk of the specimen: the two grain sizes are similar.

### Discussion

The *in-situ* data obtained demonstrate the effectiveness of using SE imaging combined with *in-situ* thermal etching to capture microstructural changes that arise at elevated temperatures. These SE images present a unique dataset that offer insight into grain growth during the ferrite to austenitic phase transition, as well as within the austenitic region. By tracking the grain growth *in-situ* at elevated temperature, observation and quantification of changes over time are facilitated without having to account for the effects of heating and cooling. Thus, *in-situ* data provide a clearer understanding of the high temperature evolution as opposed to examination after the heat treatment, which may only provide partial insight.

EBSD has also previously been used to track grain growth *in-situ*. However, due to the time limiting factor associated with EBSD scanning of a changing surface, only localized grain growth (<10 grains) has been captured (Farahani *et al.*, 2019). By combining SE imaging and thermal etching, the current study has been able to image multiple grains in a very

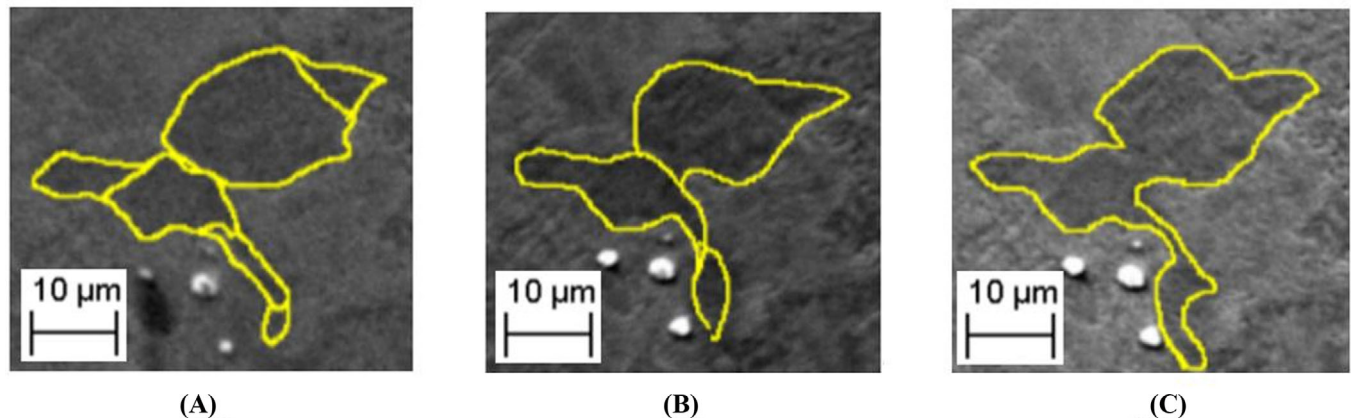
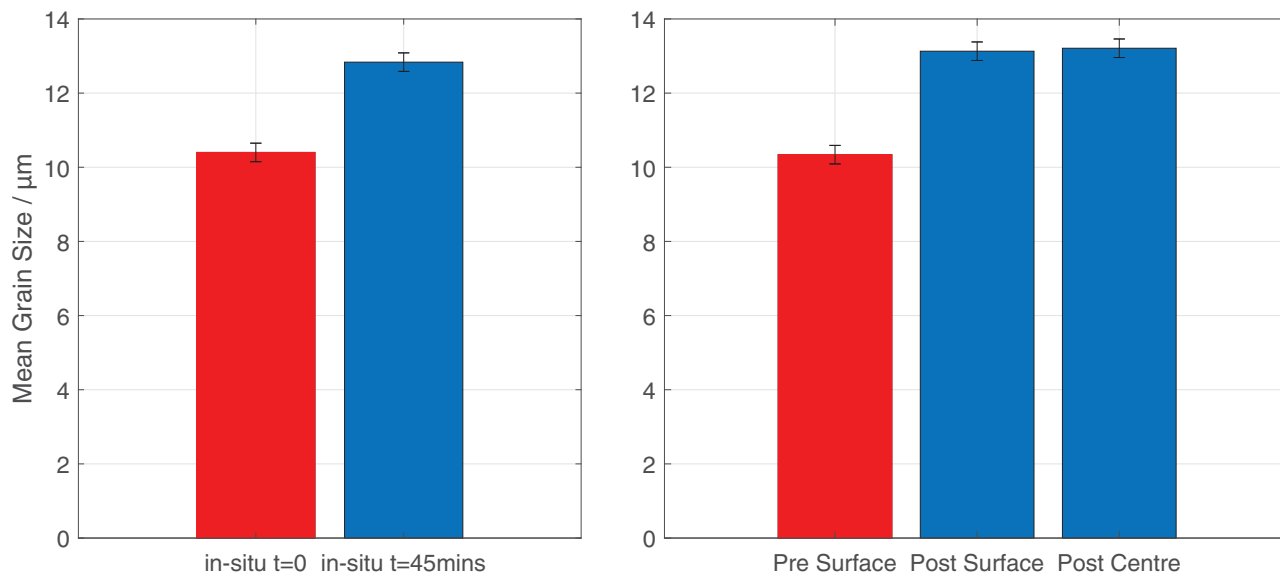


Fig. 7. SE images at 800 °C depicting a second example of abnormal grain growth from another heating cycle that was focussed on this small area where (A) 0 min, (B) 36 min and (C) 60 min.



**Fig. 8.** Comparison of grain size measured from (A) *in-situ* and (B) *ex-situ* images. The red bars indicate initial grain size upon reaching 800 °C (A) and *ex-situ* before any heating (B) indicating that there is little growth during heating. (B) Shows a comparison between bulk and surface *ex-situ* grain size post-heating, these are in good agreement, indicating that surface measurements are representative of the bulk. Comparison between the date *in-situ* at 45 min and *ex-situ* shows a small amount of grain growth on cooling. As in Figure 5, error bars of  $\pm 0.25 \mu\text{m}$  are indicated.

short space of time, providing data that are more representative of the overall grain structure. Furthermore, EBSD often requires extensive sample preparation, and during heating the surface quality has been shown to degrade over time, impeding image quality (Heard *et al.*, 2020). Conversely, a much shorter preparation time is required to facilitate *in-situ* thermal etching and the image quality does not degrade during heating.

As well as highlighting the benefits of the *in-situ* thermal etching technique, observation of microstructural changes during the heat treatment shows that grain size increases linearly with time. This phenomenon is associated with the growth of large grains at the expense of smaller ones, commonly known as abnormal grain growth (Humphreys & Hatherly, 2004), and is considered the predominant type of grain growth in this study. Given that previously documented *ex-situ* post-heat treatment data from carbon steel indicate normal non-linear grain growth (Lasagni *et al.*, 2008), this study highlights the importance of *in-situ* analysis, demonstrating the value of this technique and data.

To confirm these observations, further measurements were performed. Two examples are shown in Figures 6 and 7: Figure 6 is taken from the images shown above and Figure 7 is from further images taken over a period of 1 h at 800 °C at a higher magnification. Figure 6A shows three small grains and one larger grain nearby. After 20 min, rapid growth of the larger grain leads to the absorption of two of the smaller grains and slight growth of the third smaller grain, Figure 6B. After 45 min, Figure 6C, the larger grain has continued to grow and has also absorbed the third small grain, signifying abnor-

mal grain growth. Figure 7 shows a similar microstructural evolution.

The observation of abnormal grain growth in this case is likely attributed to some ferrite grains remaining at 800 °C, despite the phase diagram indicating a fully austenitic microstructure. As such, the ferrite grains shrink over time alongside their austenite counterpart's growth, giving the illusion of abnormal grain growth. The retainment of ferrite within this carbon steel at 800 °C has been confirmed using EBSD (Heard *et al.*, 2020) and a similar localized phenomenon of ferrite shrinking as austenite grows has been documented during cyclic phase change of steel (Farahani *et al.*, 2019). These data indicate that abnormal grain growth may be characteristic of grain evolution during the ferrite–austenite phase change as well as the fully austenitic region of carbon steel.

Due to the novelty of using the thermal etching technique *in-situ* it is important to establish any effect the sample preparation or the thermal etch itself may have on grain growth. Formation of the thermal etch occurs as a result of an equilibration of the triple junction between grain boundaries and free surfaces (Mullins, 1986). Subsequent movement of the grain boundary and, hence, the etch may, in theory, be dictated by the size of the grain. It was considered that thermal etching may result in smaller grains escaping the thermal etch more easily; whilst the grain boundary etch surrounding larger grains continued to develop due to the grain boundaries being pinned here (Mullins, 1958). As a result, larger grains could appear to absorb smaller ones due to the less pronounced original grain boundary around smaller grains combined with the pinning of larger grains rather than due

to the grain growth itself. However, comparison of the *ex-situ* data post-cooling in the bulk and surface of the specimen, as well as the *in-situ* thermal etch data taken just before cooling, indicate that the thermal etch is representative of grain boundary movement (Fig. 8). Thus, confirms that grain growth under these conditions is not affected by thermal etching.

## Conclusions

The results obtained in this study from the carbon steel specimens provide a unique dataset that gives greater insight into grain growth during the ferrite to austenite phase change and within the austenitic region. The *in-situ* data demonstrate the benefit of using SE thermal etching over EBSD or other such methods to capture grain growth *in-situ*. The data suggest that microstructural evolution during the ferrite to austenite phase change transitioning into the austenitic region of carbon steel during heat treatment at 800°C can be described by abnormal grain growth. This is based on the linearity of the results detailed in this paper as well as the observed shrinkage of ferrite grains as the austenite phase develops. Furthermore, the data also considered the possible effects of thermal etching on grain growth and confirmed that under these experimental conditions the effect was negligible. Since neither the new technique nor microstructural development has been previously observed, owing to the lack of *in-situ* high temperature data, this demonstrates the benefit of high temperature *in-situ* SEM studies on heat treatment processes.

## Acknowledgements

The authors acknowledge financial support from EPSRC. We would also like to thank Deben UK Ltd for providing both financial and technical support, in particular we thank Gary Edwards and Ed Williamson-Brown. Marzena Tkaczyk assisted with microscopy, and the technicians in the Solid Mechanics group workshop, especially Richard Duffin, at Oxford University in manufacturing specimens.

## References

- Burke, J.E. & Turnbull, D. (1952) Recrystallization and grain growth. *Prog. Met. Phys.* **3**, 220–292.
- Dossett, J.L. & Boyer, H.E. (2006) Ch 2: Fundamentals of the heat treating of steel. In *Practical Heat Treating*, pp. 9–25. ASM International, Cleveland, OH.
- Farahani, H., Zijlstra, G., Mecozzi, M.G., Ocelik, V., Hosson, J.T.M.D. & Zwaag, S.V. (2019) In situ high-temperature EBSD and 3D phase field studies of the austenite-ferrite transformation in a medium Mn steel. *Microsc. Microanal.* **25**, 639–655. <https://doi.org/10.1017/S143192761900031X>.
- Heard, R., Huber, J.E., Siviour, C., Gary Edwards, E.W.-B. & D., K. (2020) An investigation into experimental in-situ SEM imaging at high temperature. *Rev. Sci. Instrum.*
- Humphreys, F.J. & Hatherly, M. (2004) *Recrystallization and Related Annealing Phenomena*. Elsevier: Amsterdam, Netherlands.
- Lasagni, F.A., Requena, G.C. & Soppa, E.A. (2008) In situ measurements of local strain in heterogeneous materials. *Adv. Eng. Mater.* **10**, 73–78.
- Lee, S. & Lee, Y. (2008) Prediction of austenite grain growth during austenitization of low alloy steels. *Mat Des.* **29**, 1840–1844.
- Li, M., Wilkinson, D. & Patchigolla, K. (2005) Comparison of particle size distributions measured using different techniques. *Part. Sci. Technol.* **23**, 265–284.
- Methods, S.T. (2013) Standard test methods for determining average grain size 1, 1–27. ASTM International, West Conshohocken, PA. <https://doi.org/10.1520/E0112-12.1.4>.
- Mullins, W. (1958) The effect of thermal grooving on grain boundary motion. *Acta Metall.* **6**, 414–427.
- Mullins, W.W. (1986) Theory of thermal grooving. *J. App. Phys.* **28**, 333–339.
- Ngan, A.H.W. & Smallman, R.E. (2019) *Modern Physical Metallurgy*. Elsevier, Amsterdam, Netherlands.
- Schneider, C.A., Rasband, W.S. & Eliceiri, K.W. (2012) NIH Image to ImageJ: 25 years of image analysis. *Nat. Met.* **9**, 671–675.
- Sisson, R.D. (2001) Heat treatment. *Encyclopedia of Materials: Science and Technology*, pp. 3736–3741. Elsevier, Amsterdam, Netherlands. <https://doi.org/10.1016/B0-08-043152-6/00666-5>.

## Supporting Information

Additional supporting information may be found online in the Supporting Information section at the end of the article.

**Fig. S1.**  
**Fig. S2.**  
**Fig. S3.**  
**Fig. S4.**  
**Fig. S5.**  
**Fig. S6.**  
**Fig. S7.**  
**Fig. S8.**  
**Fig. S9.**  
**Fig. S10.**